

All-optical, actively Q-switched fiber laser

Robert J. Williams,* Nemanja Jovanovic, Graham D. Marshall and Michael J. Withford.

Centre for Ultrahigh bandwidth Devices for Optical Systems (CUDOS), MQ Photonics Research Centre, Department of Physics and Engineering, Macquarie University, New South Wales 2109, Australia

*robert.williams@mq.edu.au

Abstract: All-fiber lasers offer increased robustness and simplicity over other fiber laser systems. Current active Q-switching techniques for all-fiber lasers rely on electro-mechanical transducers to strain-tune an intra-cavity fiber-Bragg grating, which adds complexity and can lead to vibrational sensitivity. An all-optical technique for achieving active Q-switched operation is a more elegant approach and would maintain the inherent robustness and simplicity of an all-fiber laser system. In this work, we studied the optical tuning of a fiber-Bragg grating by resonant optical pumping and optimized it for application to active systems. We incorporated an optically-tunable fiber-Bragg grating into a fiber laser and demonstrated active Q-switching at 35 kHz with this all-optical, all-fiber laser system. We highlight the potential to operate at >300 kHz with the current embodiment. To our knowledge, this is the first demonstration of an optically-driven active Q-switch in a fiber laser. Further potential to operate at MHz frequencies is discussed.

©2010 Optical Society of America

OCIS codes: (060.3510) Fiber lasers; (060.3735) Fiber Bragg gratings; (140.3540) Q-switched lasers; (230.1150) All-optical devices; (320.2250) Femtosecond phenomena.

References and links

1. X. P. Cheng, P. Shum, C. H. Tse, R. F. Wu, W. C. Tan, M. Tang, and J. Zhang, "All-Fiber Q-Switched Ring Laser with Increased Repetition Rate," *IEEE Photon. Technol. Lett.* **20**(10), 764–766 (2008).
2. N. Jovanovic, G. D. Marshall, A. Fuerbach, G. E. Town, S. Bennetts, D. G. Lancaster, and M. J. Withford, "Highly Narrow Linewidth, CW, All-Fiber Oscillator With a Switchable Linear Polarization," *IEEE Photon. Technol. Lett.* **20**(10), 809–811 (2008).
3. N. A. Russo, R. Duchowicz, J. Mora, J. L. Cruz, and M. V. Andrés, "High-efficiency Q-switched erbium fiber laser using a Bragg grating-based modulator," *Opt. Commun.* **210**(3-6), 361–366 (2002).
4. T. V. Andersen, P. Pérez-Millán, S. R. Keiding, S. Agger, R. Duchowicz, and M. V. Andrés, "All-fiber actively Q-switched Yb-doped laser," *Opt. Commun.* **260**(1), 251–256 (2006).
5. M. Delgado-Pinar, D. Zalvidea, A. Diez, P. Perez-Millan, and M. Andres, "Q-switching of an all-fiber laser by acousto-optic modulation of a fiber Bragg grating," *Opt. Express* **14**(3), 1106–1112 (2006).
6. J. W. Arkwright, and I. M. Skinner, "An investigation of Q-switched induced quenching of the resonant nonlinearity in neodymium doped fibers," *J. Lightwave Technol.* **14**(1), 110–120 (1996).
7. J. W. Arkwright, P. Elango, T. W. Whitbread, and G. R. Atkins, "Nonlinear phase changes at 1310 nm and 1545 nm observed far from resonance in diode pumped ytterbium doped fiber," *IEEE Photon. Technol. Lett.* **8**(3), 408–410 (1996).
8. M. J. F. Digonnet, R. W. Sadowski, H. J. Shaw, and R. H. Pantell, "Experimental evidence for strong UV transition contribution in the resonant nonlinearity of doped fibers," *J. Lightwave Technol.* **15**(2), 299–303 (1997).
9. J. W. Arkwright, P. Elango, G. R. Atkins, T. Whitbread, and J. F. Digonnet, "Experimental and theoretical analysis of the resonant nonlinearity in ytterbium-doped fiber," *J. Lightwave Technol.* **16**(5), 798–806 (1998).
10. M. Janos, J. Arkwright, and Z. Brodzeli, "Low power nonlinear response of Yb³⁺-doped optical fibre Bragg gratings," *Electron. Lett.* **33**(25), 2150–2151 (1997).
11. A. Martinez, I. Y. Khrushchev, and I. Bennion, "Thermal properties of fibre Bragg gratings inscribed point-by-point by infrared femtosecond laser," *Electron. Lett.* **41**(4), 176–178 (2005).
12. N. Jovanovic, M. Åslund, A. Fuerbach, S. D. Jackson, G. D. Marshall, and M. J. Withford, "Narrow linewidth, 100 W cw Yb³⁺-doped silica fiber laser with a point-by-point Bragg grating inscribed directly into the active core," *Opt. Lett.* **32**(19), 2804–2806 (2007).

13. N. Jovanovic, J. Thomas, R. J. Williams, M. J. Steel, G. D. Marshall, A. Fuerbach, S. Nolte, A. Tünnermann, and M. J. Withford, "Polarization-dependent effects in point-by-point fiber Bragg gratings enable simple, linearly polarized fiber lasers," *Opt. Express* **17**(8), 6082–6095 (2009).
14. M. L. Åslund, N. Nemanja, N. Groothoff, J. Canning, G. D. Marshall, S. D. Jackson, A. Fuerbach, and M. J. Withford, "Optical loss mechanisms in femtosecond laser-written point-by-point fibre Bragg gratings," *Opt. Express* **16**(18), 14248–14254 (2008).
15. T. Erdogan, "Fiber grating spectra," *J. Lightwave Technol.* **15**(8), 1277–1294 (1997).
16. A. Martínez, M. Dubov, I. Khrushchev, and I. Bennion, "Direct writing of fibre Bragg gratings by femtosecond laser," *Electron. Lett.* **40**(19), 1170–1172 (2004).
17. M. K. Davis, M. J. F. Digonnet, and R. H. Pantell, "Thermal effects in doped fibers," *J. Lightwave Technol.* **16**(6), 1013–1023 (1998).
18. N. Jovanovic, A. Fuerbach, G. D. Marshall, M. J. Withford, and S. D. Jackson, "Stable high-power continuous-wave Yb³⁺-doped silica fiber laser utilizing a point-by-point inscribed fiber Bragg grating," *Opt. Lett.* **32**(11), 1486–1488 (2007).
19. P. Pérez-Millán, A. Díez, M. Andrés, D. Zalvidea, and R. Duchowicz, "Q-switched all-fiber laser based on magnetostriction modulation of a Bragg grating," *Opt. Express* **13**(13), 5046–5051 (2005).
20. M. Ams, G. D. Marshall, P. Dekker, J. A. Piper, and M. J. Withford, "Ultrafast laser written active devices," *Laser Photon. Rev.* **3**(6), 535–544 (2009).

1. Introduction

The incorporation of fiber-Bragg gratings (FBGs) into fiber lasers enables simple, compact and robust all-fiber laser cavities, eliminating the need for bulk-optic components. Further, the ability to tune the Bragg wavelength of an FBG in a fiber laser can add functionality to the all-fiber laser system, such as laser wavelength tunability, and polarization selectivity and switching [1,2]. In particular, tuning the wavelength of an FBG in an all-fiber laser cavity has been used to achieve active Q-switching [3]. Typical methods for tuning the Bragg wavelength of an FBG rely on thermal or mechanical means, such as applying strain to the FBG via an electro-mechanical transducer. These methods have limited tuning speed [1,3–5] and require the incorporation of bulky components, which is detrimental to the inherent robustness and simplicity of the all-fiber laser system.

All-optical tuning of an FBG offers potentially faster switching speeds [6], whilst maintaining the inherent robustness of an all-fiber laser. Resonantly pumping a fiber doped with rare-earth ions increases the refractive index of the core, which in accordance with the Bragg condition, shifts the Bragg wavelength of an FBG inscribed in that fiber. The refractive index shift induced by the resonant optical pumping occurs via two processes. Firstly, the excited ions experience non-radiative decay and thus directly heat the doped fiber core. Secondly, by exciting ions from the ground state to an excited state, the strength of all ground-state absorptions is diminished, while excited-state absorptions become possible and gain is made available. The intrinsic link between the real and imaginary parts of the refractive index (as described by the Kramers-Krönig relations) dictates that any change in absorption or gain, at any wavelength, induces a refractive index shift (albeit minutely small) at all wavelengths [7–9]. Thus by changing the electron-population of the energy levels of the rare-earth ions, the refractive index of the doped material is temporarily shifted. All-optical tuning of an FBG inscribed in a Yb-doped fiber has been demonstrated previously by resonantly pumping the ytterbium ions, in order to switch a passive signal [10]. However, a limited tuning range and speed was demonstrated: 17 pm at 1 Hz and 3 pm at 50 Hz. The larger tuning range at 1 Hz was attributed to heating of the fiber. Therefore, for application to active systems such as a laser system, a full understanding of- and control over the relative contributions from the optically-driven thermal and electron-population effects is required.

In order to optically tune the wavelength of an FBG, it must be directly inscribed into a fiber with resonant absorption at a wavelength which corresponds with available pump sources. Rare-earth-doped fibers are an ideal candidate as they are widely available and can be pumped with fiber-coupled diode lasers. As rare-earth-doped fibers typically have low photosensitivity, a grating inscription technique which relies upon multi-photon absorption of femtosecond laser pulses is advantageous. Further, gratings directly-written with a

femtosecond laser have proven stability at high-temperatures [11] and under intense optical fields [12], which is favourable for fiber laser applications.

In this study, we present for the first time an all-optical, active Q-switch in an all-fiber laser. We show that the tunable FBG exhibits three optical tuning regimes: a long time-scale thermally-dominated regime (limited to 1 second), an electron-population dominated regime (limited to the excited-state lifetime of 840 μs), and a fast thermal regime (limited to $\sim 3 \mu\text{s}$). By repetitively tuning this high-reflector (HR) FBG on- and off-resonance with a stabilized output-coupler (OC) FBG, the quality factor (Q) of the erbium fiber laser cavity was modulated, and the laser successfully Q-switched at repetition rates up to 35 kHz. We demonstrate that the diode driver is limiting the tuning rate, and show that the FBG is capable of tuning at frequencies greater than 300 kHz in the current embodiment. Further, we highlight potential for this system to be scaled up to repetition rates exceeding 1 MHz.

2. Grating inscription

The HR FBG was inscribed in the Yb-doped fiber using an infrared femtosecond laser and the point-by-point technique. A detailed description of this technique may be found elsewhere [13]. The following parameters were used for inscribing the grating: 200 nJ pulse energy, 30 mm grating length and a period of 1.589 μm . This grating had a third-order resonance at 1536.5 nm with reflectivity of approximately 65% (estimated from the measured transmission extinction of 14.9 dB and non-resonant loss of 1.7 dB) – and a linewidth (full-width at half-maximum reflectivity) of 65 pm. The 1.7 dB non-resonant loss was measured near the Bragg wavelength; however, as it is due to scattering out of the core by the micro-voids in the grating [14], any light which traverses the grating (resonant or non-resonant) will experience loss due to scattering. We estimated that the scattering loss at the Bragg wavelength is similar to the measured non-resonant scattering loss for this grating (the validity of such an estimation depends upon what fraction of the grating is penetrated by the reflected light). The estimated 1.7 dB scattering loss results in only 68% of the incident light remaining in the core, of which 95% (13.2 dB) is reflected; hence the estimated value of 65% for the reflectivity of this grating. The strength of the scattering loss in this grating is significantly higher than what is typically observed in standard telecommunications fiber (SMF-28e). This is mostly due to the higher ratio of overlap between the refractive index modification and the core mode: the Yb-doped fiber has a core diameter of 4 μm , whereas SMF-28e has a core diameter of 8 μm .

We also inscribed an OC FBG in an undoped fiber (Corning SMF-28e). This OC grating was inscribed using the same point-by-point technique and the following parameters: 200 nJ pulse energy, 30 mm grating length and a period of 4.242 μm . This grating had an eighth-order resonance in the C-band with reflectivity of 48% (transmission extinction of 3.6 dB including 0.36 dB scattering loss) and linewidth of 30 pm. Both of these gratings were written at a high order to reduce the coupling constant, which enabled us to write long gratings while maintaining suitable grating strengths; thus minimizing the linewidth of the gratings [15]. The ability to write strong gratings at high orders is unique to the point-by-point technique, as the size of the features remains small, regardless of grating period [16]; and gratings with low duty-cycle (ratio of feature size to grating period) have strong high-order resonances. Gratings with narrow linewidth were targeted so as to achieve the maximum change in reflectivity, given the available tuning range; and to increase the rate of change in reflectivity by increasing the slope of the band-edge.

3. Tuning of the FBG by resonant optical pumping

The tunable HR FBG was inscribed in a Yb-doped fiber with a target grating wavelength in the C-band, as ytterbium has no absorption or emission in or near the C-band. A fiber with a high ytterbium concentration (1.2 wt.%) was selected to provide a high level of resonant absorption per unit length in the fiber, and thus a large Bragg-wavelength tuning range for the grating. Figure 1 shows the setup for monitoring the FBG spectrum during continuous-wave

(CW) resonant optical pumping. The spectrum of the grating was probed in reflection using a high-resolution (3 pm) swept-wavelength system (JDS Uniphase SWS15100), and up to 200 mW of pump light from a 976 nm fiber-coupled laser diode was injected into the Yb-doped fiber via a 980/1550 nm wavelength-division multiplexer (WDM).

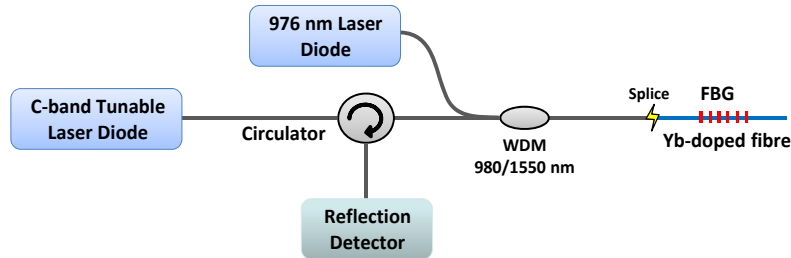


Fig. 1. Schematic of the setup for characterization of the optical tuning of the FBG.

During continuous resonant pumping, heat generated in the doped fiber core dissipates rapidly into the cladding (over a time scale of $\sim 3 \mu\text{s}$); however the rate of heat conduction out of the cladding to the surrounding air is slow. As a result, under continuous pumping heat accumulates in the cladding which can cause a significant shift in the refractive index of the core [17]. In order to suppress this slow-thermal effect we immersed the bare fiber in water to enable efficient conduction of heat from the fiber cladding. By comparing the reflection spectra obtained with the fiber in air to those obtained with the fiber in water, under identical pumping conditions, we determined the slow-thermal contribution to the total refractive index shift.

While monitoring the reflection spectrum of the FBG in the Yb-doped fiber, we resonantly pumped the Yb-doped fiber and observed the Bragg resonance shift to longer wavelengths. Fig. 2(a) shows the reflection spectrum of the grating with the fiber immersed in air: without optical pumping, with 100 mW and with 200 mW of injected optical pump power. We found that during optical tuning the Bragg reflection peak split into multiple peaks and the peak reflectivity reduced. This distortion was only temporary, and with the pump switched off the original grating spectrum was restored.

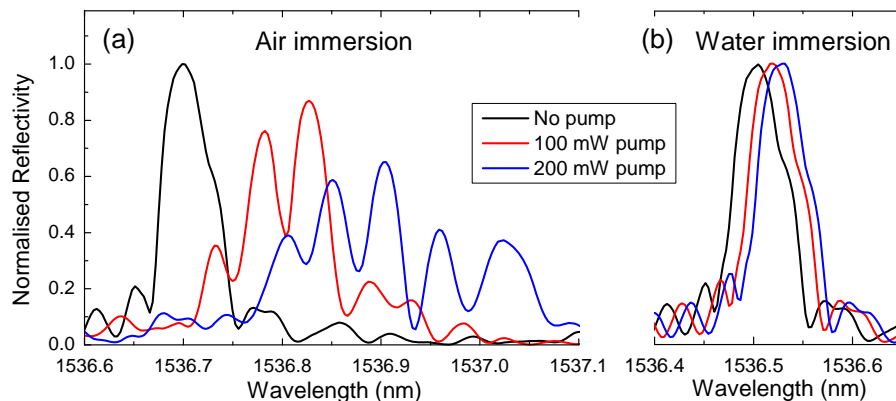


Fig. 2. Reflection spectra of the HR grating in the Yb-doped fiber, under resonant optical pumping at various powers, with the fiber immersed in air; and immersed in water.

When repeating the experiment with the fiber immersed in water, we observed a much smaller Bragg-wavelength shift (25 pm as opposed to 200 pm, again to longer wavelengths), and without any distortion of the grating spectrum or loss of peak reflectivity (see Fig. 2(b)).

We attribute the difference between the two tuning results to the slow-thermal effect described above, which is present in the case of Fig. 2(a) only. The mechanism which is giving rise to the distortion in the grating spectrum seen in Fig. 2(a) is not well understood; however we believe that scattering from the grating is generating additional, non-uniform heating within the grating region, which is affecting both the average effective index and the index contrast of the grating (thus, introducing a chirp and/or affecting the strength of the side-lobes). This splitting of the grating peak upon heating is not associated with polarization based effects, as it has been shown that the polarization dependence/birefringence of these femtosecond point-by-point gratings is due to the elliptical shape of the refractive index modification [13], which does not change with temperature. Given that the slow-thermal effect occurs over a time-scale of ~ 1 s, while operating at repetitive tuning rates greater than a few Hz the spectrum of the FBG without passive cooling would be distorted. This distortion of the grating spectrum would reduce the efficiency and stability of the fiber laser; therefore we passively cooled the grating (by water immersion) throughout the laser experiments. Without the slow-thermal effect then, the time-scales of the processes which contribute to the tuning process are $840 \mu\text{s}$ (corresponding to the excited state lifetime of ytterbium), and $3 \mu\text{s}$ (time taken for a pulse of heat to diffuse into the cladding from the fiber core).

4. All-optical, active Q-switching of the erbium fiber laser

A schematic of the fiber laser cavity is shown in Fig. 3. The cavity consisted of the HR grating in the Yb-doped fiber, the OC grating in SMF and a two-metre length of Er-doped fiber (0.14 wt.%, absorption = 12.9 dB/m @ 976 nm, core diameter $4 \mu\text{m}$) to provide gain in the C-band. Pump light at 976 nm was injected into the laser cavity through the OC grating via a 980/1550 nm WDM. A separate 976 nm diode was used to achieve optical-tuning of the HR grating by directly pumping the Yb-doped fiber. A second WDM was spliced between the HR and the cavity in order to prevent 976 nm light transmitted through the HR affecting the cavity, and vice versa. This WDM also stopped emission from the Yb-doped fiber (at ~ 1040 nm) coupling into the erbium laser cavity. Due to the extra fiber from the WDM in the cavity, the total cavity length was 5.9 m. The OC grating was placed in a heater oven and thermally tuned such that it overlapped spectrally with the HR grating.

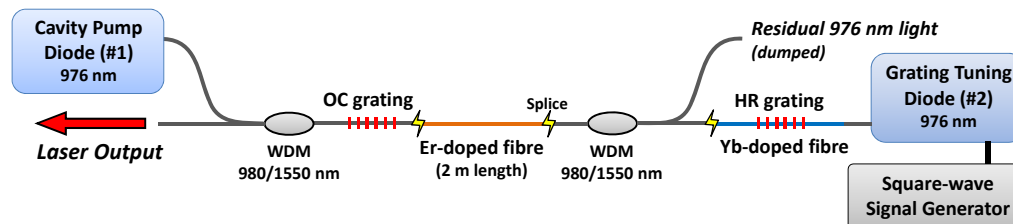


Fig. 3. Schematic diagram of the Q-switched erbium fiber laser cavity.

With the two FBG's aligned spectrally, the Er-doped fiber lased at 1536.4 nm with a narrow linewidth of 15 pm when the cavity was optically pumped from the 976 nm diode (diode #1, Fig. 3). The HR grating could be tuned off-resonance from the OC grating by injecting 40 mW of 976 nm light into the Yb-doped fiber; this resulted in a reduced Q-factor for the laser cavity. Consequently the Er-doped fiber ceased lasing, with 40 dB extinction.

In order to repetitively modulate the Q of the cavity, the HR FBG was repetitively tuned on- and off-resonance from the OC FBG by modulating the current supplied to the grating tuning diode (diode #2). This was achieved by delivering TTL control pulses from a waveform generator to the diode driver. The output of the fiber laser was monitored using an oscilloscope (2 GHz bandwidth, 4 GS/s) and an InGaAs fast photodiode (1 GHz bandwidth, 0.1 ns rise/fall time).

The erbium fiber laser operated in a stable Q-switched regime at switching frequencies between 15 and 35 kHz. Oscilloscope traces of the output of the laser at 35 kHz are shown below in Fig. 4. At frequencies below 15 kHz, the laser would not operate in a stable Q-switched regime, due to the significant cavity feedback from the gratings which is still present in the low-Q state. The pump power delivered to the cavity ranged from 40 mW at 15 kHz, to 70 mW at 35 kHz. While increasing the Q-switching frequency, an increase in the pump power delivered to the cavity was required to reach a sufficient population inversion for stable Q-switched operation.

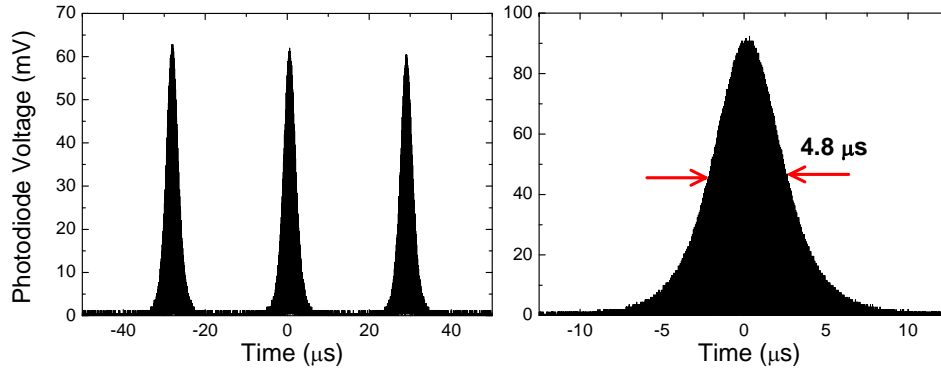


Fig. 4. Output of the Q-switched fiber laser at 35 kHz, shown on two different time-scales.

The optical spectrum of the fiber laser during Q-switched operation at 35 kHz is shown below in Fig. 5. The measured FWHM of the lasing peak is 14 pm, which is close to the resolution limit (10 pm) of the optical spectrum analyzer (Advantest Q8384). Therefore the actual spectral linewidth of the laser may be narrower.

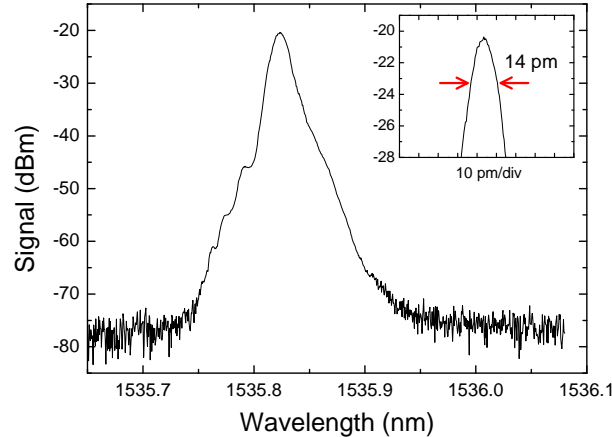


Fig. 5. Optical spectrum of the fiber laser during Q-switched operation at 35 kHz. The measurement of the optical bandwidth of the laser peak may be resolution limited.

The average power of the laser was 1.5 mW at 15 kHz, and 3.4 mW at 35 kHz. The output power of the fiber laser operating CW was 2.8 mW with 70 mW from the cavity pump diode (diode #1). The Q-switched pulse duration at FWHM was 3.1 μ s at 15 kHz, and 4.8 μ s at 35 kHz. At any fixed Q-switching frequency, we observed that increasing the pump power delivered to the cavity had the effect of simultaneously increasing the peak power and reducing the pulse duration. By calibrating oscilloscope measurements to average power

measurements, the peak output power of the laser at 35 kHz was determined to be approximately 120 mW. This is more than sufficient for our system to operate as an oscillator source in a master-oscillator power amplifier configuration, and the potential for further optimization and power scaling is highlighted in the discussion.

Considering the time-scale limits for the tuning speeds, particularly the excited-state lifetime of ytterbium (840 μ s), and the time for diffusion of heat from the core into the cladding (3 μ s), neither of these correspond to the apparent tuning frequency limit of this system at 35 kHz ($\tau = 29 \mu$ s). We observed the output of the grating tuning diode (976 nm diode #2) using the photodiode and oscilloscope, and noted that at 35 kHz the laser diode output did not fully modulate to zero. We conclude therefore, it is only the laser diode driver which is currently limiting the grating tuning frequency to 35 kHz. Given that the tuning speed limit due to the excited state lifetime of ytterbium has already been exceeded, a faster diode driver should allow grating tuning at frequencies greater than 300 kHz ($\tau = 3 \mu$ s) using the current embodiment.

While monitoring the output of the fiber laser, we observed that the Q-switched pulses periodically consisted of an underlying pulse train with full modulation (hence the ‘solid’ curves in Fig. 4). The inter-pulse spacing was measured to be 57.5 ns (which corresponds to the round-trip time for the 5.9 m cavity), and the pulse duration was measured to be 8 ns. In addition, we monitored the output of the laser without any grating tuning (i.e. no resonant pumping of the Yb-doped fiber) and discovered that the fiber laser still exhibited this pulsed output with similar pulse duration (6 ns) and identical pulse period (57.5 ns). Oscilloscope traces of the output of the fiber laser in both Q-switched and CW operating regimes are shown in Fig. 6. This self-pulsing behaviour was intermittent: pulse trains similar to those shown in Fig. 6 were present 10-20% of the time. At other times we observed either pulses at double the frequency or more complicated temporal profiles with lower peak power and higher frequency (multiples of the cavity round-trip frequency). These pulse trains (whether mode-locked-like or otherwise) were always sustained over the entire oscilloscope scan length (spanning up to 1.25 μ s). We determined that the change between mode-locked-like pulse trains and other pulse train formations occurred over sub-millisecond time-scales, by observing the changes in peak power over long time-span oscilloscope traces (due to the sampling limit of the oscilloscope, these long traces do not have sufficient data points to resolve the modulation within the cavity round-trip time). In order to verify that the photodiode is fully resolving the 6 ns pulses, we measured its response to a 100 fs pulse and found the duration of the rise/fall to be 0.6 ns (less than one tenth of the rise/fall time of the pulses in Fig. 6). Thus the oscilloscope traces shown in Fig. 6 are well within the resolution capability of the photodiode.

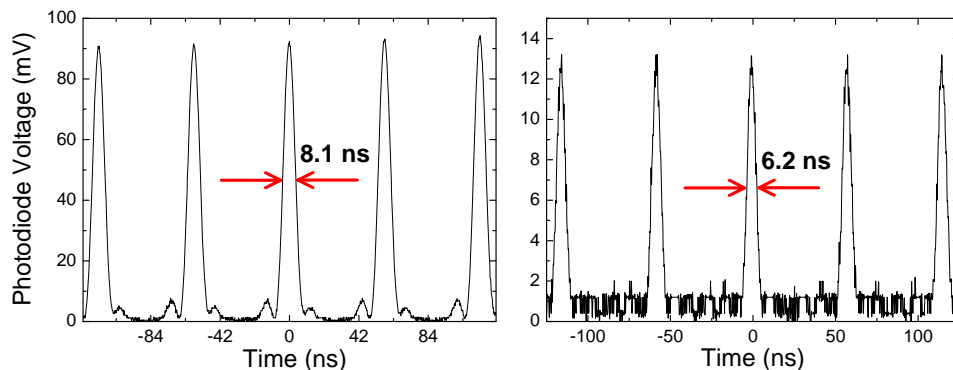


Fig. 6. Output of the fiber laser shown on a short time-scale, during Q-switched (left) and CW operation (right). For the graph on the left, the time-window shown corresponds to the peak of the Q-switched pulse-envelope.

The radio frequency (RF) spectrum of the output of the fiber laser was measured using the InGaAs photodiode and an RF spectrum analyzer (Tektronix 2792), and is shown in Fig. 7. The low-frequency peaks (Fig. 7(a)) in the Q-switched trace (black) correspond to the Q-switching frequency (35 kHz) and its harmonics. The harmonics of the Q-switching frequency are present because the modulation of the laser output at the Q-switching frequency is far from sinusoidal (see Fig. 4). The high-frequency peaks (Fig. 7(b)) occur at integer multiples of the cavity round-trip frequency (17.4 MHz). A high-resolution scan of the 17.4 MHz peak is shown in the inset on Fig. 7(b), for both the CW (red) and Q-switched case (black). In the Q-switched trace we observe sidebands positioned at 35 kHz intervals on either side of the 17.4 MHz peak, which correspond to the Q-switched modulation of the underlying pulse trains (including the fundamental Q-switch frequency and its harmonics).

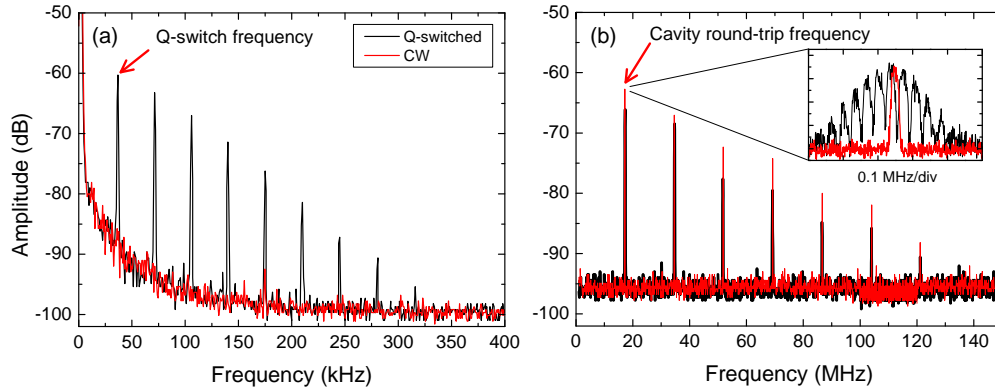


Fig. 7. Radio frequency spectrum of the output of the fiber laser operating Q-switched at 35 kHz (black) and CW (red). The 35 kHz peak and harmonics are observed during Q-switched operation (a). Peaks at the cavity round-trip frequency (17.4 MHz) and harmonics are observed during both Q-switched and CW operation (b). A high-resolution scan is also shown at 17.4 MHz (inset, b), showing the 35 kHz sidebands in the Q-switched case.

As the scan time for the RF spectrum analyzer is much slower than the time taken for the laser output to change between mode-locked-like pulse trains and higher-frequency modulations, we would expect that the mode-locked-like pulse trains alone would generate a similar RF spectrum to what is observed in Fig. 7(b), even though they are not consistently present. As the laser output observed on the oscilloscope also showed pulse-trains/modulation at multiples of the cavity round-trip frequency, these will also contribute to the peaks observed at these frequencies. By monitoring the RF spectrum at 17.4 and 34.8 MHz, we determined that the threshold pump power for CW self-pulsing is equal to the CW lasing threshold. The strength and narrow linewidth of the peaks and the low noise floor in the RF spectrum confirm the stability of the Q-switching in this laser system, and the presence of strong modulation at the cavity round-trip frequency.

5. Discussion

In this work, an optically-tunable FBG was incorporated into a fiber laser system for the first time. We used the laser output as well as observation of the grating spectrum during optical tuning, to investigate the contributing mechanisms to the tuning process. In doing so, we observed temporary detrimental effects on the grating spectrum and confirmed that these were due to the accumulation of heat in the fiber cladding. We subsequently eliminated this slow-thermal effect with passive cooling and observed optical tuning of the FBG without any degradation of the grating spectrum. This result is important for any active system with an FBG inscribed directly in an active fiber, as the efficiency and stability of the system depends upon the feedback from the FBG; which is in agreement with observations noted in [18]. We

also demonstrated grating tuning at 35 kHz, which is faster than the reciprocal of the excited state lifetime of the ytterbium ions; therefore we have shown optical-tuning based on the direct heating of the fiber core only, which has potential to operate at frequencies greater than 300 kHz.

By incorporating the optically-tunable FBG into an erbium fiber laser we achieved optically-driven, active Q-switching of an all-fiber laser for the first time. Previous methods for actively Q-switching all-fiber lasers mainly consist of strain-tuning an FBG via an electrically-driven transducer, such as a piezoelectric transducer (PZT) [1,3,5] or a magnetostrictive element [4,19]. This requires that the electro-mechanical element be bonded to the fiber, which reduces the robustness and simplicity of the all-fiber laser and can lead to heating of the FBG during Q-switched operation, and instability of the laser system [19]. The range of frequencies at which these Q-switches can operate is limited by the electro-mechanical element. In the case of a Q-switched all-fiber laser based on strain-tuning an FBG with a PZT element, the Q-switching frequencies were limited to integer factors of the mechanical resonance of the PZT, which in this case was 18.5 kHz [3]. Magnetostrictive elements are less restricted in this sense as they have a relatively flat frequency response over a large range, and continuous tuning of the Q-switching frequency has been demonstrated up to 200 kHz [4]. As mentioned above, our demonstration of Q-switching using the all-optical technique at 35 kHz shows that optical-tuning of the grating is possible at repetition frequencies greater than 300 kHz, using an appropriate diode driver. Furthermore, if the Yb-doped fiber can be made to lase, then the excited-state lifetime of the ytterbium ions will be reduced by stimulated emission, and the refractive index shift due to the electron-population may be able to tune the FBG at frequencies exceeding 1 MHz [6].

The duration of the Q-switched pulses from our system ranged from approximately 3 to 5 μ s, which is slightly longer than previous results for all-fiber Q-switched lasers (ranging typically from 180 ns to 3 μ s) [1,3,4,19]. Additionally, the efficiency of the laser is low: the average output power of the laser at 35 kHz Q-switching frequency was 3.4 mW, with approximately 70 mW pump power. However, there is significant potential for improving the pulse duration, peak power and efficiency of this laser. Currently there is approximately 3.5 m of undoped fiber in the cavity from the WDM, there are multiple splice losses in the cavity between mode-mismatched fibers, and there is significant scattering loss in the HR FBG (\sim 1.7 dB). Reducing the cavity length, reducing the cavity losses and optimizing the output coupling will result in shorter Q-switched pulses with higher peak power, and a more efficient laser. Additionally, in order to scale the system to high power, a fiber amplification stage could easily be spliced onto the output of the laser, without losing the benefits of an all-fiber laser cavity.

We observed that during both Q-switched and CW operation, the laser output periodically consisted of an underlying pulse-train with full modulation and an inter-pulse spacing corresponding to the round-trip time of the cavity. The RF spectrum of the laser showed strong peaks at integer multiples of the cavity round-trip frequency of the laser, with low background noise, during both CW and Q-switched operation. We determined that the threshold for CW self-pulsing is equal to the threshold for CW lasing in this system. These results indicate that this self-pulsing behaviour is due to mode-beating in the laser and that only a few modes (less than 10) may be lasing at a time, in which case the bandwidth of the laser will be less than 2 pm. We are currently investigating this further. Self-pulsing at the cavity round-trip frequency has been observed in other actively Q-switched all-fiber lasers [5,19]; however this is the first report where the self-pulsing fully modulated the fiber-laser output during the Q-switched pulse (others report up to \sim 60% modulation of the output power). This is also the first report to our knowledge of CW self-pulsing in an all-fiber laser.

6. Conclusion

We have presented what we believe to be the first all-optical, active Q-switch in a fiber laser system; as well as the first optically-tunable FBG in a fiber laser cavity (where the optical tuning is independent of the cavity pumping). The Q-switched pulse duration of this system is comparable to that of other all-fiber Q-switched lasers [1,3,19] with scope for further improvement. We have shown that the Q-switching mechanism has potential to operate at frequencies of at least 300 kHz, which exceeds the demonstrated capability of other all-fiber, actively Q-switched lasers [1,4,5].

We have demonstrated that optically-tunable FBGs can be effectively employed in active fiber laser systems to achieve active Q-switching; and we believe that these may also provide rapid wavelength tunability, polarization switching (see [2]), and other functionality to all-fiber lasers. However, fibers with higher doping concentrations will likely be required to increase the tuning range, such as Yb-doped phosphate or phosphosilicate fibers. This work also highlights potential for application in direct-write active devices [20].

Acknowledgements

This work was produced with the assistance of the Australian Research Council under the ARC Centres of Excellence and LIEF programs. The authors would like to thank Dr David Spence for useful discussions regarding self-pulsing and mode-beating, and Professor Benjamin Eggleton of the University of Sydney for useful discussions regarding the methods used in this work.